

Reinforcement Learning the Chromatic Symmetric Function

Gergely Bérczi ^{*} Jonas Klüver [†]

Abstract

We propose a conjectural counting formula for the coefficients of the chromatic symmetric function of unit interval graphs using reinforcement learning. The formula counts specific disjoint cycle-tuples in the graphs, referred to as Eschers, which satisfy certain concatenation conditions. These conditions are identified by a reinforcement learning model and are independent of the particular unit interval graph, resulting a universal counting expression.

1 Introduction

The study of proper graph colorings is a fundamental area in graph theory and theoretical computer science. For a given graph G , the number of ways to color its vertices with n colors, such that no two adjacent vertices share the same color, is given by the chromatic polynomial $\chi_G(n)$. The chromatic polynomial exhibits several intriguing properties, including log-concavity, a celebrated result established by Huh [4]. The chromatic symmetric function, a multi-variable generalization of the chromatic polynomial, was introduced by Richard Stanley [8], who formulated several deep conjectures in the 1990's regarding its algebraic properties. This symmetric function is connected to various fields, including topology, statistical mechanics, representation theory and algebraic geometry, and holds a central position in algebraic combinatorics and graph theory.

The goal of this paper is to study the chromatic symmetric function using machine learning techniques. Motivated by the Stanley-Stembridge positivity conjecture [10, 8], our main result is a conjectured counting formula for coefficients of the elementary symmetric function expansion of the chromatic symmetric function, suggested by deep reinforcement learning models.

Let G be a finite graph, with $V(G)$ representing its vertices and $E(G)$ representing its edges.

Definition 1.1. A **proper coloring** c of G is a function $c : V \rightarrow \mathbb{N}$, where no two adjacent vertices share the same color.

^{*}Department of Mathematics, Aarhus University, email: gergely.berczi@math.au.dk

[†]Department of Mathematics, Aarhus University, email: jonas.kluever@gmail.com

For a given coloring c , we can associate a monomial:

$$x_c = \prod_{v \in V} x_{c(v)},$$

where x_1, x_2, \dots are commuting variables. Let $\Pi(G)$ denote the set of all proper colorings of G , and let $\Lambda \subset \mathbf{Z}[x_1, x_2, \dots]$ denote the ring of symmetric functions in the infinite set of variables x_1, x_2, \dots .

Definition 1.2. The **chromatic symmetric function** $X_G \in \Lambda$ of a graph G is defined as the sum of the monomials x_c over all proper colorings c of G :

$$X_G = \sum_{c \in \Pi(G)} x_c.$$

Remark 1.3. One could consider a finite but sufficiently large number of colors r , which would lead to $X_G \in \Lambda_r$, the set of symmetric polynomials in r variables. Although this slightly complicates notation, it does not alter the results.

Definition 1.4. The m -th **elementary symmetric function** e_m is defined as:

$$e_m = \sum_{i_1 < i_2 < \dots < i_m} x_{i_1} x_{i_2} \dots x_{i_m},$$

where $i_1, \dots, i_m \in \mathbb{N}$. Given a partition $\lambda = (\lambda_1 \geq \lambda_2 \geq \dots \geq \lambda_k)$, we define the elementary symmetric function e_λ as $e_\lambda = \prod_{i=1}^k e_{\lambda_i}$. These functions form a basis of Λ .

Definition 1.5. A symmetric function $X \in \Lambda$ is **e-positive** if it can be written as a non-negative linear combination of elementary symmetric functions.

For example, the chromatic symmetric function of K_n , the complete graph on n vertices, is $X_{K_n} = n!e_n$, which is e-positive.

Definition 1.6. The **incomparability graph** $\text{inc}(P)$ of a poset P is the graph whose vertices are the elements of P , and two vertices are adjacent if they are incomparable in P .

Definition 1.7. A poset P is said to be $(a+b)$ -free if it does not contain a chain of length a and a chain of length b that are mutually incomparable.

Definition 1.8. A **unit interval order** (UIO) is a poset that is isomorphic to a finite subset of $U \subset \mathbb{R}$, where u and $w \in U$ are incomparable if and only if $|u - w| < 1$.

Theorem 1.9 (Scott-Suppes [6]). *A finite poset P is a UIO if and only if it is $2+2$ -free and $3+1$ -free.*

Stanley and Stembridge [10, 8] proposed the following positivity conjecture.

Conjecture 1.10 (Stanley-Stembridge [10]). *If P is a $3 + 1$ -free poset, then $X_{inc(P)}$ is e -positive.*

The Stanley-Stembridge suggests that for the incomparability graph of any $3 + 1$ -free poset P , the coefficients c_λ in the expansion

$$X_G = \sum_{\lambda} c_\lambda e_\lambda,$$

are non-negative for all partitions λ . It has been computationally verified for posets with up to 20 elements [1]. In [7] Sharesahian and Wachs introduced a refined version of the chromatic symmetric functions, and conjectured that these chromatic quasi-symmetric functions are also e -positive.

In 2013, Guay-Paquet [1] showed that it is enough to prove the Stanley-Stembridge conjecture for the case where the poset is both $3 + 1$ -free and $2 + 2$ -free, i.e., for unit interval orders.

Theorem 1.11 (Guay-Paquet [1]). *Let P be a $3 + 1$ -free poset. Then, $X_{inc(P)}$ is a convex combination of the chromatic symmetric functions*

$$\{X_{inc(P')} \mid P' \text{ is both } 3 + 1\text{-free and } 2 + 2\text{-free}\}.$$

Shortly before submitting our preprint, we became aware of Hikita’s work [3], which presents a probabilistic interpretation of the Stanley coefficients and establishes the e -positivity conjecture. In contrast, our results offer a fundamentally different interpretation of these coefficients, discovered through the application of machine learning techniques.

Acknowledgments

We thank Andras Szenes for introducing us to this problem. We are greatly indebted to Ádám Zsolt Wagner, whose expertise in machine learning profoundly shaped this paper. The first author was supported by DFF 40296 grant of the Danish Independent Research Fund.

2 The main results

In this paper, instead of using supervised learning models to study the Stanley coefficients directly, we follow a more sophisticated learning strategy, which was motivated by recent work of Szenes and Rok [11]. This work suggests that the Stanley coefficients should count specific cycle-tuples within the UIO. This method offers two key advantages:

1. It provides an exact counting interpretation of the coefficients.
2. It yields a universal formula, as the cycles we count depend only on the partition λ , rather than on the specific UIO.

The strategy in a nutshell is the following: given a partition $\lambda = (\lambda_1, \dots, \lambda_s)$ the Stanley coefficient c_λ is given by the count of λ -Eschers in the UIO satisfying certain splitting and insertion conditions. We use a reinforcement learning agent to identify the correct conditions. Hence the central objects are Eschers, which are cycles of a certain type in the UIO graph. Given two unit intervals u_1 and u_2 on the real line, their relative positions can fall into one of three categories:

1. u_1 intersects u_2 ,
2. $u_1 \cap u_2 = \emptyset$ and u_1 is to the left of u_2 ,
3. $u_1 \cap u_2 = \emptyset$ and u_1 is to the right of u_2 .

Following [11], we will use the notation $u_1 \prec u_2$ for case (2), $u_1 \succ u_2$ for case (3), and $u_1 \rightarrow u_2$ if either case (1) or case (2) holds.

Definition 2.1. Let U be a unit interval order with intervals u_0, \dots, u_{n-1} . The **area sequence of U** is the unique increasing sequence $a_U = (a_0 \leq \dots \leq a_{n-1})$ where

1. $0 \leq a_i \leq i$ is integer
2. $u_i \sim u_j$ if and only if $i \geq a_j$.

Remark 2.2. The number of UIOs of length n is equal to the number of increasing integer sequences satisfying condition (1), which is the Catalan number $C_n = \frac{1}{n+1} \binom{2n}{n}$, and the number coefficients of the chromatic symmetric function X^U is the number of partitions of n , which we denote by \mathcal{P}_n . Here's a table for small number of vertices:

# Vertices	# UIOs, C_n	# Coeffs, $ \mathcal{P}_n $
2	2	2
3	5	3
4	14	5
5	42	7
6	132	11
7	429	15
8	1430	22
9	4862	30
20	6564120420	627

For small UIOs it is feasible to compute all coefficients and verify their non-negativity. Computation of the Stanley coefficients is based on a combinatorial formula of Theorem 3.16, using the Stanley G-homomorphism. However, as the table suggests, the complexity grows rapidly. Calculating these coefficients becomes both memory- and time-intensive. The conjecture has been verified for UIOs of up to length 20 [1].

Definition 2.3. We call a sequence $[v_0, v_1, \dots, v_{k-1}]$ of distinct elements from U a k -**Escher** if the relation

$$v_0 \rightarrow v_1 \rightarrow \dots \rightarrow v_{k-1} \rightarrow v_0$$

holds. We will denote by E_k^U the set of k -Eschers in U . For a pair of integers k, l we denote by $E_{k,l}^U$ the set of disjoint (k, l) **Escher pairs**:

$$E_{k,l} = \{(v, w) \in E_k^U \times E_l^U : v \cap w = \emptyset\}$$

We adapt the same notation for longer **Escher-tuples**.

The operation of cyclic permutation on sequences is denoted by ζ :

$$\zeta : [v_0, v_1, \dots, v_{k-1}] \mapsto [v_1, v_2, \dots, v_{k-1}, v_0].$$

By applying powers of ζ to a k -Escher, we generate $k - 1$ new k -Eschers. Since all the resulting sequences are equivalent, we refer to this group of sequences as a "cyclic Escher" to represent the isomorphism class of sequences related by ζ . An Escher, then, is a cyclic Escher with a chosen starting point. For a given escher u we let u^v denoted the escher equivalent to u , starting at $v \in u$. Additionally, for a k -Escher, we treat the index set as integers modulo k , so that, for instance, $u_0 = u_k$.

Our starting point is the following observation of Szenes-Rok [11], following Stanley [8]. The general formula using G homomorphism will be given in the next section.

Proposition 2.4 (Stanley, Szenes-Rok). *Let U be a UIO of length $n \geq k + l$. The Stanley coefficient corresponding to $\lambda = (k, l)$ is $c_{(k,l)}^U = \#E_{k,l}^U - \#E_{k+l}^U$.*

Definition 2.5. Let U be a unit interval order (UIO) of length n , and let $v = [v_0, \dots, v_{k-1}] \in E_k^U$ be a k -Escher. Fix a positive integer $l \leq k$. If there exists an $m \in \mathbb{N}$ such that

$$v_{m+1} \rightarrow v_{m+2} \rightarrow \dots \rightarrow v_{m+l} \rightarrow v_{m+1}$$

and

$$v_0 \rightarrow \dots \rightarrow v_m \rightarrow v_{m+l+1} \rightarrow \dots \rightarrow v_{k-1}$$

holds, then we call $[v_{m+1}, \dots, v_{m+l}]$ a **valid l -subescher** of v . We call such m a **splitting point** or **subescher starting point** of v . We denote by $\mathbf{S}(v, l)$ the set of splitting points, and if this is nonempty then we let $\mathbf{SEStart}(v, l)$ denote the first (smallest non-negative) splitting point (SEStart for Sub-Escher Start), and $\mathbf{SEEnd}(v, l) = \mathbf{SEStart}(v, l) + l$.

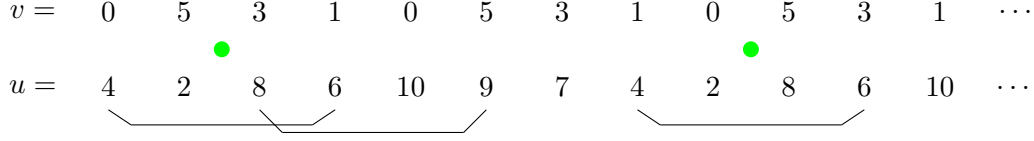
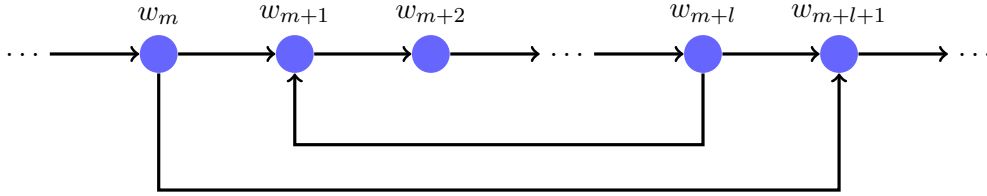


Figure 1: Insertion points and sub-Eschers for the Escher pair $u = [4, 2, 8, 6, 10, 9, 7]$, $v = [0, 5, 3, 1]$ in the UIO $U = (0, 0, 1, 1, 2, 3, 3, 4, 6, 7, 9)$. Green dots indicate insertion points (i.e. $2 \rightarrow 3$ and $5 \rightarrow 8$ in U , and underbrace indicates length 4 sub-Eschers in u).

In short, a valid subescher of length l is a subescher such that the remaining part of v still forms an Escher, illustrated as follows:



Proposition 2.6. [11], Proposition 4.5. Any $k+l$ -Escher has at least one valid k -subescher.

Definition 2.7. Let $u = [u_0, \dots, u_{k-1}] \in E_k^U$ and $v = [v_0, \dots, v_{l-1}] \in E_l^U$ be disjoint subeschers of length k, l respectively, that is, $(u, v) \in E_{k,l}^U$ is a (k, l) Escher-pair. We call $i \in \mathbb{Z}$ an **insertion point** for (u, v) if $u_i \rightarrow v_{i+1}$ and $v_i \rightarrow u_{i+1}$ holds. In this case we can concatenate u and v to get a length $k+l$ escher $u+_i v$ as follows:

1. for $i = 0, \dots, k-1$

$$u+_i v = [u_0, \dots, u_i, v_{i+1}, \dots, v_{i+l}, u_{i+1}, \dots, u_{k-1}]$$

2. for $i \geq k$ we define

$$u+_i v = [u_q, \dots, u_i, v_{i+1}, \dots, v_{i+l}, u_{i+1}, \dots, u_{q+k-1}]$$

where $q \in (i-k, i]$ is chosen s.t. $k|q$.

Denote the set of insertion points by $\mathbf{I}(u, v)$, and if this is nonempty, then the first (smallest non-negative) insertion point by $\mathbf{FirstIns}(u, v)$.

Example 2.8. Let U be the UIO with 11 intervals given by the area sequence $U = (0, 0, 1, 1, 2, 3, 3, 4, 6, 7, 9)$ as in Figure 1. Let

$$u = [4, 2, 8, 6, 10, 9, 7], v = [0, 5, 3, 1]$$

forming a $(7, 4)$ Escher-pair $(u, v) \in E_{4,3}^U$. We put (u, v) periodically under each other with a period $lcm(7, 4) = 28$ as in Figure 1. We indicated by green array the insertion points.

In contrast to Proposition 2.6, there are Escher pairs that have no insertion points. Hence Proposition 2.4 intuitively suggests that for a fixed pair (k, l) the Stanley coefficient $c_{(k,l)}^U$ counts (k, l) Escher-pairs in U which cannot be concatenated to an $(k + l)$ -Escher. The technical difficulty lies in handling Eschers as linear, not cyclic objects.

To follow this intuition, to an Escher pair $(u, v) \in E_{k,l}^U$ we associate a 3-dimensional rational vector, which we call the **core vector**, defined as the function

$$\tau^2 : E_{k,l}^U \rightarrow \mathbb{Q}^4$$

$$\tau^2(u, v) = \begin{cases} (0, -1, -1, -0.5) & \text{if } \mathbf{I}(u, v) = \emptyset, \\ (0, \mathbf{SEStart}(u, l), \mathbf{SEEnd}(u, l), \mathbf{FirstIns}(u, v) + 0.5) & \text{if } \mathbf{I}(u, v) \neq \emptyset \ \& \ 0 < \mathbf{SEStart}(u, l), \\ (0, -1, -1, \mathbf{FirstIns}(u, v) + 1.5) & \text{if } \mathbf{I}(u, v) \neq \emptyset \ \& \ 0 = \mathbf{SEStart}(u, l). \end{cases}$$

By Proposition 2.6 all cases are covered. We call τ^2 the **core representation** for Escher pairs. We spent considerable time to come up with the right core coordinates, and generalise the core representation to Escher tuples of length 3 and higher. We see that the second and third coordinates are integers, the fourth coordinate is always half-integer, this is crucial in the RL model. We will denote the i th coordinate with $\tau_i^2(u, v)$, and simply refer to them as 0, **SEStart**, **SEEnd**, **FirstIns**, but keeping in mind their more sophisticated definition.

The intuition is that the numerical relationship among the core coordinates characterizes those (k, l) Escher pairs which do not concatenate to a $(k + l)$ Escher in Proposition 2.4. Our first result supports this intuition.

ML Theorem 1 (Counting formula for pairs). *For any UIO of length at least $k + l$*

$$c_{(k,l)}^U \geq \#\{(u, v) \in E_{k,l}^U : \tau_3^2(u, v) < \tau_4^2(u, v)\} \quad (1)$$

and equality holds for all UIOs when $\lambda = (k, k)$. Moreover, equality holds for almost all UIOs even when $k \neq l$: for a fixed (k, l) the mismatch ratio is less than 0.5%, see Remark 2.9 for explanation.

Remark 2.9. 1. Table 1 illustrates Theorem 1. We observe that for pairs $(k, l) \neq (5, 3), (5, 4)$ we get perfect matching and equality in (1). For $\lambda = (5, 3)$, there is a mismatch in (1) for only 1 out of 429 UIOs. This exceptional UIO is

$$U = (0, 0, 1, 2, 3, 4, 5, 6)$$

which does not exhibit any obvious unusual properties, making it unclear why the mismatch occurs specifically with this UIO.

2. More notably, from Table 1 the sum of the 429 Stanley coefficients is 52,500, while the total absolute error is just 1.

3. This phenomenon highlights why proving a counting formula is so challenging: we encounter extremely rare exceptional UIOs with minimal mismatches, yet there is no apparent explanation for their occurrence.

We can illustrate the conditions in (1) as a graph, whose vertices are the cores of the representation, and an oriented edge from `core1` to `core2` means that $core1 < core2$, see Figure 2.

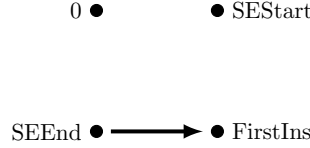


Figure 2: Condition graph for Escher pairs

For a triple $\lambda = (k, l, m)$, the idea is that the Stanley coefficient $c_{(k,l,m)}^U$ should count the (k, l, m) Escher tuples where no two tuples concatenate at the deepest level—in other words, any two tuples remain non-concatenated. For a triple $(u, v, w) \in E_{k,l,m}^U$, we use the core coordinates for the pairs (u, v) , (u, w) , and (v, w) . However, if u and v do concatenate, then we need to store the core coordinates for the pair (uv, w) , (uw, v) and (vw, u) as well. This results in a total of 19 core coordinates as follows:

$$\tau^3 : E_{k,l,m}^U \rightarrow \mathbb{Q}^{19}$$

$$\tau^3(u, v, w) = (0, \tau^2(u, v)[1:], \tau^2(v, w)[1:], \tau^2(u, w)[1:], \tilde{\tau}^2(uv, w), \tilde{\tau}^2(uw, v), \tilde{\tau}^2(vw, u))$$

where

1. $\tau^2(u, v)[1:]$ stands for the last 3 coordinates of $\tau^2(u, v)$, that is, we drop the 0 from the beginning.
2. the definition of $\tilde{\tau}^2$ is quite subtle due to the cases where u and v do not concatenate, making the cores involving uv undefined or irrelevant. We let

$$\tilde{\tau}^2(uv, w) = \begin{cases} (-1, -1, -0.5) & \text{if } \mathbf{I}(u, v) = \emptyset \\ \tau^2(u +_i v, w)[1:] & \text{if } \mathbf{FirstIns}(u, v) = i \end{cases} \quad (2)$$

For a more concise and descriptive reference we use the following shorthand notation: for a triple $(u, v, w) \in E_{(k,l,m)}^U$ we put

$$\mathbf{SEStart}(u, v) = \mathbf{SEStart}(u, |v|) \text{ and } \mathbf{SEEnd}(u, v) = \mathbf{SEEnd}(u, |v|).$$

So the notations for the 19 core coordinates are

$$\begin{aligned} \tau_3(u, v, w) = & (0, \mathbf{SEStart}(u, v), \mathbf{SEEnd}(u, v), \mathbf{FirstIns}(u, v), \\ & \mathbf{SEStart}(v, w), \mathbf{SEEnd}(v, w), \mathbf{FirstIns}(v, w), \\ & \mathbf{SEStart}(u, w), \mathbf{SEEnd}(u, w), \mathbf{FirstIns}(u, w), \\ & \mathbf{SEStart}(uv, w), \mathbf{SEEnd}(uv, w), \mathbf{FirstIns}(uv, w), \\ & \mathbf{SEStart}(uw, v), \mathbf{SEEnd}(uw, v), \mathbf{FirstIns}(uw, v), \\ & \mathbf{SEStart}(vw, u), \mathbf{SEEnd}(vw, u), \mathbf{FirstIns}(vw, u)) \end{aligned}$$

The condition graph we are looking for has maximum 19 vertices, and our RL agent found the following

ML Theorem 2 (Counting formula for triples). 1. For a triple (k, l, m) with $k \geq l \geq m$

$$c_{(k,l,m)}^U \approx \# \left\{ (u, v, w) \in E_{k,l,l}^U : \begin{array}{l} \mathbf{SEEnd}(u, v) < \mathbf{FirstIns}(u, v), \\ \mathbf{SEEnd}(u, w) < \mathbf{FirstIns}(u, w), \\ \mathbf{SEEnd}(v, w) < \mathbf{FirstIns}(v, w) \end{array} \right\}$$

where \approx means that the mismatch ratio is $< 3\%$ and total absolute error ratio less than 1% (see Table 2).

2. For $\lambda = (k, l, l)$ with $k \geq l$ we have equality above, and our counting formula gives the Stanley coefficient (see Table 2)
3. There is a modified canonical model which gives lower bound for all triples (k, l, m) with $k \geq l \geq m$ (see Table 3):

$$c_{(k,l,m)}^U \geq \# \left\{ (u, v, w) \in E_{k,l,m}^U : \begin{array}{l} 0 \geq \mathbf{SEStart}(u, v), 0 \geq \mathbf{SEStart}(u, w), 0 \geq \mathbf{SEStart}(v, w) \\ \mathbf{SEEnd}(u, v) < \mathbf{FirstIns}(u, v), \\ \mathbf{SEEnd}(u, w) < \mathbf{FirstIns}(u, w), \\ \mathbf{SEEnd}(v, w) < \mathbf{FirstIns}(v, w) \end{array} \right\}$$

The corresponding condition graphs are shown in Figure 3.

We concluded similar results for quadruples, see Table 4,5 and we summarize our findings as

ML Theorem 3 (General counting formula). Let $\lambda = (\lambda_1 \geq \lambda_2 \geq \dots \geq \lambda_r)$ be a partition then

- 1.

$$c_\lambda^U \approx \# \{ (u_1, \dots, u_r) \in E_\lambda^U : \mathbf{SEEnd}(u_i, u_j) < \mathbf{FirstIns}(u_i, u_j) \text{ for all } 1 \leq i < j \leq r \}$$

where \approx means that the mismatch ratio is $< 1\%$ for most λ 's

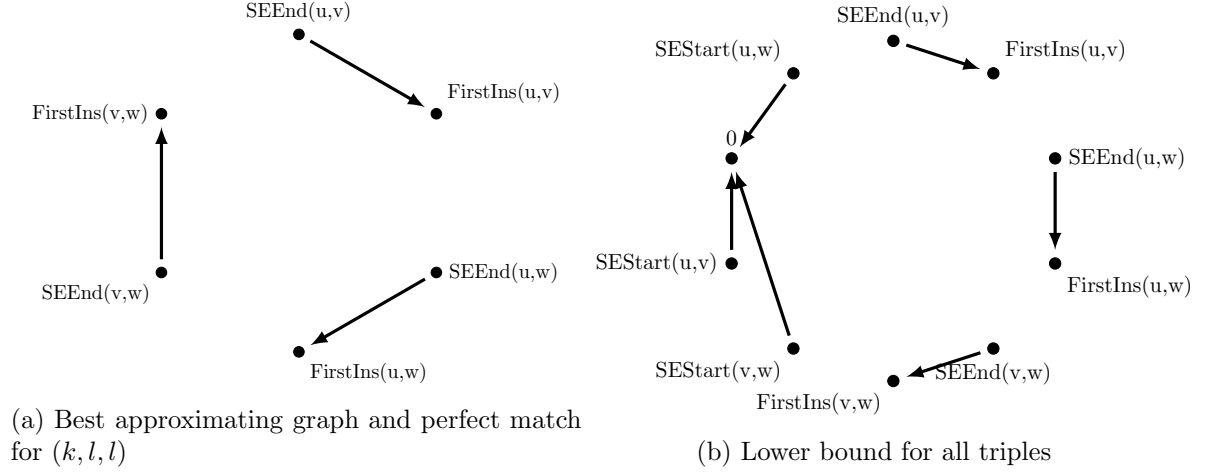


Figure 3: The condition graphs for Escher triples

2. For $\lambda = (k, l, l, \dots, l)$ with $k \geq l$ we have equality above, and our counting formula gives the Stanley coefficient.
3. Slight modification provides lower bound for the coefficients:

$$c_\lambda^U \geq \# \left\{ (u_1, \dots, u_r) \in E_\lambda^U : \begin{array}{l} \mathbf{SEEnd}(u_i, u_j) < \mathbf{FirstIns}(u_i, u_j) \text{ for all } 1 \leq i < j \leq r \\ 0 \geq \mathbf{SEStart}(u_i, u_j) \text{ for all } 1 \leq i < j \leq r \end{array} \right\}$$

3 Mathematical background

3.1 Stanley's G-homomorphism

Let $\Lambda \subset \mathbb{Z}[x_1, x_2, \dots]$ denote the ring of symmetric functions in the variables x_1, x_2, \dots , generated as an algebra by the elementary symmetric functions $\{e_i : i = 0, 1, \dots\}$ defined in Definition 1.4, and as a \mathbb{Z} -module by $\{e_\lambda\}$. Given a finite graph G with vertices $V = \{v_1, \dots, v_n\}$, let $\Lambda_G = \mathbb{Z}[v_1, \dots, v_n]$, be the polynomial ring on the vertices. Stanley's G-homomorphism $\rho_G : \Lambda \rightarrow \Lambda_G$ is defined as the unique ring-homomorphism s.t.

$$\rho_G(e_i) = \sum_{\substack{S \subseteq V \\ S \text{ is empty, } |S|=i}} \prod_{v \in S} v$$

where the sum is taken over all subgraphs on i vertices without edges. For $f \in \Lambda$ we set $f^G = \rho_G(f)$.

Example 3.1. Let G be a finite graph on n vertices. Then $e_1^G = \sum_{v \in G} v$, if furthermore G has at least 1 edge, then $e_n^G = 0$. For a partition $\lambda = (\lambda_1 \geq \lambda_2 \geq \dots \geq \lambda_r)$ we have

$$e_\lambda^G = \prod_{i=1}^r e_i^G,$$

Definition 3.2. Let $\alpha : V \rightarrow \mathbb{N}$ be a function assigning a nonnegative integer to each vertex of G .

1. We use the shorthand notation $\mathbf{v}^\alpha = \prod_{v \in V} v^{\alpha(v)} \in \Lambda_G$, and for $f \in \Lambda$, let $[f^G, \mathbf{v}^\alpha]$ denote the coefficient of the monomial \mathbf{v}^α in f^G .
2. We denote by G^α , the graph where each vertex v_i is replaced by the complete graph $K_{\alpha(i)}$, and for $i \neq j$ a vertex from $K_{\alpha(i)}$ is connected to a vertex from $K_{\alpha(j)}$ if and only if v_i and v_j are connected by an edge in G .

Note that the function $f \mapsto [f^G, \mathbf{v}^\alpha]$ is linear, but not a ring-homomorphism: given a graph G with at least one edge we have $[e_i^G, \mathbf{v}^\alpha] = 0$ for all $i \in \mathbb{N}$ but $[((e_1)^n)^G, \mathbf{v}^\alpha] = n!$.

Definition 3.3. We have other canonical bases of symmetric functions:

1. Denote by p_m the m -th power sum symmetric function $p_m = \sum_{i \in \mathbb{N}} x_i^m$. Given a partition $\lambda = (\lambda_1 \geq \lambda_2 \geq \dots \geq \lambda_k)$, we define the **power sum symmetric function**

$$p_\lambda = \prod_{i=1}^k p_{\lambda_i}.$$

2. Given a partition $\lambda = (\lambda_1 \geq \lambda_2 \geq \dots \geq \lambda_k)$, we define the **monomial symmetric function**

$$m_\lambda = \sum_{i_1 < i_2 < \dots < i_k} \sum_{\sigma \in S_k(\lambda)} x_{i_1}^{\lambda_1} x_{i_2}^{\lambda_2} \dots x_{i_k}^{\lambda_k},$$

where the inner sum is taken over the set of all permutations of the sequence λ , denoted by $S_k(\lambda)$.

3. For a partition $\lambda = (\lambda_1 \geq \lambda_2 \geq \dots \geq \lambda_k)$, define the **Schur functions** as

$$s_\lambda = \det(e_{\lambda_i^* + j - i})_{i,j},$$

where λ^* is the conjugate partition to λ .

The sets $\{p_\lambda\}, \{m_\lambda\}, \{s_\lambda\}$ form three basis of the ring Λ of symmetric functions.

Proposition 3.4 (Stanley [9]). *Let $\mathbf{x} = (x_1, x_2, \dots)$ denote an infinite set of variables and $\mathbf{v} = (v_1, \dots, v_n)$ the variables given by the vertices of G . Let*

$$T(\mathbf{x}, \mathbf{v}) = \sum_{\lambda} e_{\lambda}(\mathbf{x}) m_{\lambda}^G(\mathbf{v})$$

then

$$[T(\mathbf{x}, \mathbf{v}), \mathbf{v}^{\alpha}] \prod_{v \in V} \alpha(v)! = X_{G^{\alpha}}$$

Using Proposition 3.4, Stanley proved [9] that the simultaneous e-positivity of a large class of graphs is equivalent to monomial positivity of m_{λ}^G for all partitions:

Theorem 3.5. (Stanley) *For every finite graph G we have*

1. $X_{G^{\alpha}}$ is s-positive for every $\alpha : V(G) \rightarrow \mathbb{N} \iff s_{\lambda}^G \in \mathbb{N}[V(G)]$ for every partition λ
2. $X_{G^{\alpha}}$ is e-positive for every $\alpha : V(G) \rightarrow \mathbb{N} \iff m_{\lambda}^G \in \mathbb{N}[V(G)]$ for every partition λ

Proof. Let \mathbf{x}, \mathbf{y} denote 2 infinite sets of independent variables. The Cauchy product

$$C(\mathbf{x}, \mathbf{y}) = \prod_{i,j} (1 + x_i y_j)$$

yields the identities [5, (4.2'), (4.3')]

$$\sum_{\lambda} s_{\lambda}(\mathbf{x}) s_{\lambda^*}(\mathbf{y}) = \sum_{\lambda} m_{\lambda}(\mathbf{x}) e_{\lambda}(\mathbf{y}) = \sum_{\lambda} e_{\lambda}(\mathbf{x}) m_{\lambda}(\mathbf{y})$$

with the sums over all partitions of any length. By viewing only \mathbf{y} as the indeterminates and \mathbf{x} as constant we can apply the G-homomorphism and get

$$\sum_{\lambda} s_{\lambda}(\mathbf{x}) s_{\lambda^*}^G(\mathbf{v}) = \sum_{\lambda} m_{\lambda}(\mathbf{x}) e_{\lambda}^G(\mathbf{v}) = \sum_{\lambda} e_{\lambda}(\mathbf{x}) m_{\lambda}^G(\mathbf{v})$$

Using Proposition 3.4 gives

$$X_{G^{\alpha}} = \left(\prod_{v \in V} \alpha(v)! \right) \sum_{\lambda} e_{\lambda}(\mathbf{x}) [m_{\lambda}^G(\mathbf{v}), \mathbf{v}^{\alpha}] = \left(\prod_{v \in V} \alpha(v)! \right) \sum_{\lambda} s_{\lambda}(\mathbf{x}) [s_{\lambda^*}^G(\mathbf{v}), \mathbf{v}^{\alpha}]$$

■

If the chromatic polynomial is $X^G = \sum_{\lambda} c_{\lambda}^G e_{\lambda}$, then using Proposition 3.4 with $\alpha \equiv 1$, we get

$$c_{\lambda}^G = [m_{\lambda}^G, v_1 \cdot v_2 \cdot \dots \cdot v_n]$$

for any partition λ . In particular, the Stanley conjecture follows if

$$[m_{\lambda}^U, v_1 \cdot v_2 \cdot \dots \cdot v_n] \geq 0$$

for all unit interval order graphs U .

3.2 Eschers

Let U be a unit interval graph on N vertices. Recall the notation $E_\lambda^U = \{\lambda\text{-Escher tuples in } U\}$, and $X^U = \sum_\lambda c_\lambda^U e_\lambda$ is the Stanley chromatic function. Let us work out the coefficient c_N^U first.

Definition 3.6. Let U be a UIO. We call a sequence $w = [w_1, \dots, w_k]$ of distinct elements of U correct if

- $w_i \not\sim w_{i+1}$ for $i = 1, 2, \dots, k-1$ and
- for each $j = 2, \dots, k$, there exists $i < j$ such that $w_i \sim w_j$.

We denote by C_k^U the set of length- k correct sequences in U . For a partition $\lambda = (\lambda_1, \dots, \lambda_r)$ we denote by C_λ^U the set of length $\lambda_1 + \dots + \lambda_r$ -sequences in U , which are concatenations of a length- λ_1 -correct sequence with a length- λ_2 -correct sequence with a ... with a length- λ_r -correct sequence.

Theorem 3.7 (Szenes-Rok, [11]). *For any $k \leq N$*

$$p_k^U = \sum_{w \in C_k^U} w_1 \cdot \dots \cdot w_k \in \mathbb{N}[U]$$

Furthermore for any partition $\lambda = (\lambda_1, \dots, \lambda_r)$ we have

$$p_\lambda^U = \prod_{i=1}^r p_{\lambda_i}^U = \prod_{i=1}^r \sum_{w \in C_{\lambda_i}^U} w_1 \cdot \dots \cdot w_{\lambda_i} = \sum_{w \in C_\lambda^U} w_1 \cdot w_1 \cdot \dots \cdot w_N \quad (3)$$

This leads to

Proposition 3.8. $c_N^U = \#C_N^U \geq 0$

Proof. Using the identity $p_N = \sum_{i=1}^{\infty} x_i^N = m_N$ we apply the G -homomorphism to get $m_N^U = p_N^U$ and thus $c_N^U = [m_N^U, v_1 \cdot v_2 \cdot \dots \cdot v_N] = \#C_N^U \geq 0$ by 3.7. \blacksquare

Theorem 3.9 (Szenes-Rok, [11]). *Let U be a UIO on N intervals. Then $\#E_k^U = \#C_k^U$ for any $k \leq N$ and hence by Proposition 3.8*

$$c_N^U = \#E_N^U$$

3.3 Escher-pairs

Let $\lambda = (n, k)$ be a fixed pair with $n + k \leq N$. Apply the G -homomorphism to the identity

$$m_{(n,k)} = p_n p_k - p_{n+k}$$

in Λ and we get

$$m_{(n,k)}^U = p_n^U p_k^U - p_{n+k}^U$$

Using Theorem 3.9 we get

$$c_{(n,k)}^U = \#E_n^U \cdot \#E_k^U - \#E_{n+k}^U \quad (4)$$

In fact, it is not hard to see that we can work with disjoint Escher pairs, hence we arrive at

Theorem 3.10 (Stanley coeff formula for pairs).

$$c_{(n,k)}^U = \#E_{n,k}^U - \#E_{n+k}^U$$

To prove non-negativity of $c_{(n,k)}^U$, Szenes and Rok [11] construct an injective function

$$\phi : E_{n+k}^U \rightarrow E_{(n,k)}^U$$

We go through the key steps of the proof to show the intuition behind our core representations τ_k . The idea is to find two functions

$$\phi : E_{n+k}^U \rightarrow E_{(n,k)}^U, \quad \psi : E_{n,k}^U \rightarrow E_{n+k}^U \text{ such that } \psi \circ \phi = id$$

Let $w \in E_{n+k}^U$. By Proposition 2.6, w has a first splitting point $L = \mathbf{SEStart}(w, k)$, so that $v = [w_{L+1}, \dots, w_{L+k}]$ and $u = [w_{L+k+1}, \dots, w_{L+k+n}]$ are k and n Eschers respectively. It's natural to define ϕ as $w \mapsto (u, v)$, but the problem is that it is not always the case that (u, v) has an insertion point which we could use to concatenate u and v to define ψ . But it turns out that there are cyclic permutations $u' \in [u]$, $v' \in [v]$ s.t. (u', v') has an insertion point. Namely, pick $u' \in [u]$ s.t. $u'_L = u_{n-1}$ and $v' \in [v]$ s.t. $v'_L = v_{k-1}$, i.e.

$$u'_i = u_{i+n-L-1} \text{ and } v'_i = v_{i+k-L-1} \quad (5)$$

Define

$$\phi : E_{n+k}^U \rightarrow E_{n,k}^U, \quad \phi(w) = (u', v')$$

. Then we prove that

Lemma 3.11. *For any $w \in E_{n+k}^U$ the pair $(u', v') = \phi(w)$ has an insertion point at $L = \mathbf{SEStart}(w, k)$. Furthermore $u' +_L v' \in [w]$*

Proof. u' and v' can be concatenated at L since

$$\begin{aligned} u'_L &= u_{n-1} = w_{L+k+n} = w_L \rightarrow w_{L+1} = v_0 = v'_{L+1}, \\ v'_L &= v_{k-1} = w_{L+k} \rightarrow w_{L+k+1} = u_0 = u'_{L+1} \end{aligned}$$

and $u' +_L v'$ is the same cycle-type as w since

$$\begin{aligned} u' +_L v' &= [u'_q, \dots, u'_L, v'_{L+1}, \dots, v'_{L+k}, u'_{L+1}, \dots, u'_{q-1}] \\ &= [u_{q-L-1}, \dots, u_{n-1}, v_0, \dots, v_{k-1}, u_0, \dots, u_{q-L-2}] \\ &\sim [v_0, \dots, v_{k-1}, u_0, \dots, u_{n-1}] = [w_{L+1}, \dots, w_{L+k}, w_{L+k+1}, \dots, w_{L+k+n}] \in [w] \end{aligned}$$

■

Now let's try to construct ψ , we already know $u' +_L v' \sim w$, so for them to be equal, we only need their starting point to be the same. The first element of $u' +_L v'$ will by definition always be from u' , i.e. from u , but depending on where the k -subescher v starts in w , it could be that $w_0 \in v$. So if we want to recover w from u' and v' we need to change the starting point of $u' +_L v'$ in one of the 2 cases.

To find the criterion to decide in what case we are, note that $u_i = w_{L+k+1+i}$ for $0 \leq i < n$ and $v_i = w_{L+1+i}$ for $0 \leq i < k$. So $w_0 \in u$ can only happen if $u_{n-L-1} = w_0$, so the criterion is $n - L - 1 \in [0, n - 1] \iff 0 \leq L \leq n - 1$. Similarly we get $w_0 \in v \iff v_{n+k-L-1} = w_0 \iff n \leq L < n + k$.

If $L < n$ we get by (5) that

$$(u' +_L v', L)_0 = u'_0 = u_{L-n-1} = w_0 \Rightarrow u' +_L v' = w$$

If $L \geq n$ we get by (5) that

$$(u' +_L v')_0^{v'_n} = v'_n = v_{n+k-L-1} = w_0 \Rightarrow (u' +_L v')^{v'_n} = w$$

Our discussion can be summarized in

Lemma 3.12. *Let $w \in E_{n+k}, (u, v) = \phi(w)$ and $L = FS(w)$ then*

$$w = \begin{cases} u +_L v & \text{if } L < n \\ (u +_L v)^{v_n} & \text{if } L \geq n \end{cases}$$

This inspires our definition of ψ :

Definition 3.13. Fix some dummy $w_0 \in E_{n+k}$, define $\psi : E_{n,k} \rightarrow E_{n+k}$ as

$$\psi((u, v)) = \begin{cases} w_0 & \text{if } (u, v) \text{ has no insertion point} \\ u +_{FI(u,v)} v & \text{if } FI(u, v) < n \\ (u +_{FI(u,v)} v)^{v_n} & \text{if } FI(u, v) \geq n \end{cases}$$

Theorem 3.14. $\psi \circ \phi$ is the identity

We have the following characterization of $E_{n,k} \setminus im(\phi)$:

Corollary 3.15. The complement of the image of ϕ can be seen as

$$im(\phi)^C = \{(u, v) \in E_{n,k} \mid (u, v) \text{ has no insertion point or } \phi \circ \psi((u, v)) \neq (u, v)\}$$

Proof. Let $(u, v) \in im(\phi)$, pick $w \in E_{n+k}$ s.t. $\phi(w) = (u, v)$ then $\phi \circ \psi(u, v) = \phi(w) = (u, v)$. On the other hand $\phi \circ \psi((u, v)) = (u, v) \in im(\phi)$. \blacksquare

3.4 Escher-tuples

Let $\lambda = (\lambda_1, \dots, \lambda_r)$ a partition. Using Stanley's G -homomorphism, we can come up with a similar formula for c_λ^U using Escher-tuples as in to that in Theorem 3.10. Indeed, the symmetric polynomial $m_{(\lambda_1, \dots, \lambda_r)} \in \Lambda$ can be uniquely written in the total sum basis as

$$m_{(\lambda_1, \dots, \lambda_r)} = \sum_{\tau} d_{\tau}^{\lambda} p_{\tau}$$

with integer coefficients d_{τ}^{λ} . Applying the G -homomorphism we obtain

$$m_{(\lambda_1, \dots, \lambda_r)}^U = \sum_{\tau} d_{\tau}^{\lambda} p_{\tau}^U$$

and by Theorem 3.9 again, we get

Theorem 3.16 (Stanley coeff formula).

$$c_{\lambda}^U = \sum_{\tau} d_{\tau}^{\lambda} \cdot \#E_{\tau}^U.$$

We state this formula for triple and quadruple partitions as corollary, for reference.

Corollary 3.17 (Stanley triple coeff formula).

$$c_{(n,k,l)}^U = \#E_{(n,k,l)}^U + 2 \cdot \#E_{(n+k+l)}^U - \#E_{(n+k,l)}^U - \#E_{(n+l,k)}^U - \#E_{(k+l,n)}^U$$

Using the pair formula in Theorem 3.10 we can rewrite this as

$$c_{(n,k,l)}^U = \#E_{(n,k,l)}^U + \#E_{(n+k+l)}^U - c_{(n+k,l)}^U - c_{(n+l,k)}^U - c_{(k+l,n)}^U$$

Corollary 3.18 (Stanley quadruple coeff formula).

$$\begin{aligned} c_{(n,k,l,m)}^U = & \#E_{(n,k,l,m)}^U - \\ & - \#E_{(n+k,l,m)}^U - \#E_{(n+l,k,m)}^U - \#E_{(n+m,k,l)}^U - \#E_{(k+l,n,m)}^U - \#E_{(k+m,n,l)}^U - \#E_{(l+m,n,k)}^U + \\ & + \#E_{(n+k,l+m)}^U + \#E_{(n+l,k+m)}^U + \#E_{(n+m,k+l)}^U + \\ & + 2 * (\#E_{(n+k+l,m)}^U + \#E_{(n+k+m,l)}^U + \#E_{(n+l+m,k)}^U + \#E_{(k+l+m,n)}^U) - \\ & - 6 * \#E_{(n,k,l,m)}^U \end{aligned}$$

4 Machine Learning

The message of Theorem 3.16 is that the Stanley coefficient c_λ should count λ -Escher tuples satisfying some specific splitting and concatenation properties. Following the conventions and notations of §2, for any partition $\lambda = (\lambda_1, \dots, \lambda_r)$ we define the core representation

$$\tau_\lambda : E_\lambda^U \rightarrow \mathbb{Q}^{\xi(\lambda)}$$

which roughly sends a λ -Escher-tuple $\mathbf{u} = (u_1, \dots, u_r)$ to its core vector of dimension $\xi(\lambda)$, collecting **SEStart**(v, w), **SEEnd**(v, w) and **FirstIns**(v, w) points for all possible v, w pairs which come from concatenation of Eschers in the tuple. Coordinates of the core vector are called cores, and the number $\xi(\lambda) = \xi(|\lambda|)$ will depend only on the length of λ .

As we have seen in §2, the delicate issue is how to define those coordinates of the representation where there is no concatenation point. For example, how do we define **SEStart**($u_i u_j, u_k$), **SEEnd**($u_i u_j, u_k$), and **FirstIns**($u_i u_j, u_k$) when $\mathbf{I}(u_i, u_j) = \emptyset$, and therefore we can not concatenate u_i with u_j ?

$$\tau^r : E_{(\lambda_1, \dots, \lambda_r)}^U \rightarrow \mathbb{Q}^{\xi(\lambda)}$$

$$\tau^r(u_1, \dots, u_r) = (0, \tau^2(u_i, u_j)[1:], \tilde{\tau}^2(u_i u_j, u_k))$$

where $1 \leq i < j < k \leq r$ and we do not add further core coordinates, corresponding to longer concatenations, because (according to our experiments) they do not result in better condition graphs. For the definition of $\tau^2(u_i, u_j)[1:]$ and $\tilde{\tau}^2(u_i u_j, u_k)$ see (2).

We call a permutation of the $\xi(\lambda)$ entries of the core vector a sorting permutation, if it moves the entries to descending order. The sorting permutation is not unique in case there are repeated entries. For a permutation $\tau \in S_{\xi(\lambda)}$ we denote by $E_\lambda^U(\tau)$ the set of λ -tuples whose sorting permutation is τ .

Following extensive experiments with Gurobi Software [2] involving Escher tuples, triples and quadruples, we arrived to the following surprising conjecture, which says that the Stanley coefficients are determined by the sorting orders, not the actual value of the core coordinates.

Conjecture 4.1. *For any partition λ there is a set of sorting orders*

$$T_\lambda = \{\tau_1, \dots, \tau_{N(\lambda)}\},$$

independent of U , such that

$$c_\lambda^U = \#(E_\lambda^U(\tau_1) \cup \dots \cup E_\lambda^U(\tau_N)).$$

That is, the Stanley coefficient c_λ counts the number of λ -Escher tuples with sorting core order in T_λ . We say that T_λ characterises the Stanley coefficient c_λ

While attempting to describe the Stanley coefficients through the use of characterizing sets, several significant challenges arose, which we can summarise as follows.

1. **Exponential Growth of Characterizing Sets:** The size $N(\lambda)$ of the characterizing set increases drastically, even for small cases like triples. This rapid growth makes the analysis computationally difficult and inefficient.
2. **Dependence on Partition Structure:** The characterizing set is not solely determined by the length $|\lambda|$ of the partition but depends intricately on the specific structure of the partition λ . This complicates generalization and creates additional complexity when dealing with different partitions of the same length.
3. **Subset-Sum Problem and Decision Tree Complexity:** Identifying the appropriate characterizing sets can be viewed as a specialized instance of the subset-sum problem in combinatorics, which is known to be NP-hard. Attempts to represent these sets using decision trees have resulted in extremely complicated and large structures. These trees are not only cumbersome to compute but also impractical to use for further theoretical analysis.

Due to these challenges, we were unable to find a workable description of characterizing sets even for partitions of length 3, which highlights the difficulty in scaling this approach for more general cases.

Our strategy, instead, was to describe T_λ as a set of partitions $\tau \in S_{l(\lambda)}$ satisfying a Boolean expressions of the form

$$\text{Condition}_1 \text{ OR } \text{Condition}_2 \text{ OR } \dots \text{ OR } \text{Condition}_r,$$

where each condition has the form

$$\text{Condition} = \tau(i_1) < \tau(j_1) \text{ AND } \dots \text{ AND } \tau(i_s) < \tau(j_s)$$

We encoded Condition_i as a graph G_λ^i on the vertices $\{1, \dots, \xi(\lambda)\}$, with a directed edge from i_t to j_t for $t = 1, \dots, r$, and call

$$G_\lambda = G_\lambda^1 \cup \dots \cup G_\lambda^r$$

a condition graph. Due to the coding practice, we often refer to the number of Conditions as the number of rows of our condition graph.

4.1 The RL algorithm

Our policy-based reinforcement learning model is an adapted version of the cross-entropy method for graphs, as developed by Adam Zsolt Wagner [12]. The deep NN learns a probability distribution that guides the agent’s decisions during graph construction.

The RL agent learns to identify optimal condition graphs. Specifically, after fixing the number of rows r , we initialized r copies G_1, \dots, G_r of the empty graph on $\xi(\lambda)$ vertices. The edge set of each graph G_i is ordered as e_1^i, \dots, e_m^i , where $m = \binom{\xi(\lambda)}{2}$, and we defined a sequential edge ordering across the r graphs as follows:

$$e_1^1, e_1^2, \dots, e_1^r, e_2^1, e_2^2, \dots, e_2^r, \dots, e_m^r.$$

At each step, the RL agent processes this ordered list of edges and adds the corresponding edge to the current graph G_λ based on a policy learned by a deep neural network (NN). Each run consists of $r \cdot \binom{\xi(\lambda)}{2}$ steps, where the agent decides whether or not to add each edge.

The neural network takes two binary vectors as input:

1. Game Turn Vector: A binary vector that tracks the number of moves made in the current game, with all entries set to 0 except the one corresponding to the current turn set to 1.
2. Graph State Vector: A binary vector representing the current state of the graph. The i -th entry is set to 1 if the edge corresponding to that entry was added during the i -th turn, and 0 otherwise.

The output of the NN is a probability distribution over $\{0, 1\}$. The agent samples from this distribution to make its decision for the current step: if the sampled value is 1, the corresponding edge is added to the graph.

The RL agent learns the game by running batches of agents through a series of complete games. After each game, the agents are evaluated based on their performance, and the top-performing individuals—typically the top 10%—are selected to update the neural network. It is important to note that there is a single shared NN used by all agents during training. The input-output pairs (game state at step i , decision at step i) from the top agents are used to adjust the NN parameters via the cross-entropy method. This selection mechanism encourages the model to replicate the successful behaviors of the best-performing agents.

Additionally, a small percentage of the all-time best agents are retained throughout training and used in future updates. This approach ensures that the NN continues to learn from historically strong strategies, thereby improving the likelihood of finding optimal solutions.

We modified Wagner’s cross-entropy method at the following crucial points:

1. Multi-Type Edges: While Wagner’s method uses binary edge choices, our graphs allow edges to take multiple types. Accordingly, we modify the probability distribution to output values in $\{0, \dots, K - 1\}$, where K is the number of possible edge types. Furthermore we use categorical cross-entropy instead of binary cross-entropy

for training and our Graph State Vector uses one-hot encoding for every K consecutive bits to encode a value in $\{0, \dots, K - 1\}$. Concretely we use $K=3$ to express that either the source vertex is smaller than the target vertex, or greater equal to the target vertex or that the relation is irrelevant.

2. **Edge Selection:** Not every two vertices have a meaningful relationship, so out of the full $r \cdot m$ edges we will only pick some and reduce the size of our ordered list of edges. Our selection was heavily guided by mathematical intuition and was necessary since the training otherwise would be stuck in local minima when using all edges. Reducing the edges also improves the running time of the algorithm linearly.
3. **State Memorization:** To speed up computation, we cache the scores of previously encountered graph states. This allows us to reuse scores instead of recomputing them when the same graph configuration is encountered again, significantly reducing computational overhead in later stages of training.

5 Implementation

The complete python code implementation can be found at

<https://github.com/berczig/PositivityConjectures>.

To generate the necessary training data for our model, we follow a multi-step process involving combinatorial generation and brute-force classification. The key steps are outlined below:

Step 1: Generating UIO graphs We first generate all UIOs of length N , where $N \leq 10$. For each UIO, we construct the associated incomparability graph. This graph is represented as an $N \times N$ matrix, where for each pair (i, j) , the matrix entry specifies the relation between u_i and u_j for the UIO (u_0, \dots, u_{N-1}) . The incomparability graph is used as a structural feature for downstream tasks.

Step 2: Generating λ -Eschers Using a brute-force search approach, we generate all possible tuples of UIOs and identify which tuples correspond to Escher structures. The process systematically checks each tuple to determine whether or not it satisfies the Escher condition. This classification serves as a binary label for the dataset.

Step 3: Calculating Coefficients c_λ^U For each valid UIO U and partition λ , we calculate the corresponding coefficient c_λ^U using Theorem 3.10 and Corollary 3.17, 3.18. The generated dataset includes coefficients for all tuples (λ, U) , where $\lambda = (\lambda_1, \dots, \lambda_r)$ and $U = (u_1, \dots, u_N)$, subject to the constraints:

$$2 \leq r \leq 4, \quad \lambda_1 + \dots + \lambda_r \leq N \leq 10.$$

With a C++ implementation, we successfully generated a dataset of approximately 100,000 tuples, enabling efficient training of our model.

Step 4: Calculating Cores and Core-Types For each UIO U , we compute all its core vectors $\tau_\lambda(E_\lambda^U)$, classifying all core vectors into emerging core-types. The dataset stores the distinct core-types along with their respective counts. Specifically, we iterate over all cores, and when a new core-type is encountered, we store it. If a core-type has been observed previously, we simply increment the counter associated with that core-type.

The number of core-types is significantly smaller than the total number of λ -Escher tuples, which enables optimization. When evaluating a condition graph, we iterate over the distinct core-types, summing the contributions of all matching core-types with their respective multiplicities:

$$c_G^U = \sum_{\substack{w \in E_\lambda^U \\ \tau^r(w) \text{ satisfies } G}} 1 = \sum_{\substack{w \in \tau^r(E_\lambda^U) \\ w \text{ satisfies } G}} \# \text{cores with core-type } w. \quad (6)$$

By reducing the evaluation to core-types, we can streamline computation, especially for large-scale experiments.

In our model we calculate all coefficients simultaneously, this is faster since two UIOs can share the same core-type and by batching the computation we only have to check if the core-type satisfies a condition graph once. We collect all distinct core-types

$$B = \bigcup_{\text{UIO } U, |U|=n} \tau^r(E_\lambda^U)$$

and calculate the coefficient prediction vector (recall C_n stands for the n th Catalan number, which is the number of length n UIOs)

$$c_G = \sum_{\substack{w \in B \\ w \text{ satisfies } G}} (\# \text{cores with core-type } w \text{ in } U_1, \dots, \# \text{cores with core-type } w \text{ in } U_{C_n}). \quad (7)$$

5.1 Score Function

Given a partition λ we apply the same score function for all UIOs of the same size, i.e. having the same number of intervals. Let $0 < n$ denote the number of intervals, and C_n , the n 'th Catalan number, which is the number of UIOs of size n . We let $x \in \mathbb{N}^{C_n}$ denote the predicted coefficients vector and let $y \in \mathbb{N}^{C_n}$ denote the true Stanley coefficients vector. Then we define the score function as

$$\text{score}_1(x) = -\|x - y\|_1 - \mathbf{1}(\text{has trivial row}) \cdot 10000 - \text{num_edges} \cdot \text{EdgePenalty} \quad (8)$$

In the modified version where we search for a lower bound of the Stanley coefficient, we set the score to be a large negative number in case there is a UIO with where predicted coeff > true coeff:

$$score_2(x) = \begin{cases} -5000, & \text{if } x_i > y_i, \text{ for any } i \geq 0 \\ score_1(x), & \text{else} \end{cases} \quad (9)$$

Notice, we have opted for a negative score function because our objective is to maximize the score, with the optimal value set at 0.

5.2 Hyperparameters

Wagner’s implementation includes several hyperparameters that govern the learning process, such as the learning rate, the number of graphs per batch, and the selection percentage of the top-performing individuals, among others. We retained most of these hyperparameters in our experiments. The learning rate was primarily set to either 0.01 or 0.05. After conducting numerous experiments, we found that a batch size of 600 graphs yielded comparable results to a larger batch size of 1500 graphs, making it a more efficient choice. Moreover, we employed one-hot encoding for graph representations.

A significant speedup in our approach was achieved by focusing on a random subset of the UIOs. If the algorithm fails to find a condition graph for this subset, it is unlikely to succeed when evaluated against all UIOs. This strategic reduction not only enhances computational efficiency but also improves the likelihood of successful evaluations, and allowed us to work with longer UIOs.

5.3 Results

This section presents the results obtained using the RL agent, summarized in tables. Each table provides an overview of the mismatches between the Stanley coefficients and the counts associated with a given condition graph. The mismatches are evaluated in two different ways, in individual tables

1. **Tables with number of correctly predicted UIOs:** The entry A/B indicates that, out of a total of B UIOs, the condition graph correctly predicts the coefficient for A UIOs.
2. **Tables with total absolute error:** The entry A/B means that the total sum of the Stanley coefficients for all UIOs is B , while

$$A = \sum_U |\text{predicted coeff for U} - \text{real coeff for U}|$$

Entries highlighted in blue indicate that the predicted coefficient is less than or equal to the actual coefficient for all UIOs of the given length, meaning the condition graph provides a lower bound for the coefficients. In contrast, entries highlighted in orange indicate the opposite: the predicted coefficient is greater or equal to the real for all UIOs. Magenta entries indicate mixed results, and non-highlighted entries indicate perfect match.

Total absolute error/sum of real coefficients for all UIO						
Partition \ UIO length	4	5	6	7	8	9
(2, 2)	0/12	0/192	0/1876	0/14496	0/97436	0/597056
(3, 1)	0/30	0/440	0/4044	0/29852	0/193626	0/1152912
(3, 2)		0/75	0/1446	0/16517	0/145828	0/1100405
(4, 1)		0/259	0/4590	0/49193	0/413056	0/2992325
(3, 3)			0/414	0/9630	0/128796	0/1302006
(4, 2)			0/746	0/16532	0/213152	0/2093462
(5, 1)			0/2820	0/58706	0/719904	0/6784258
(4, 3)				0/3903	0/103326	0/1550199
(5, 2)				0/9595	0/240366	0/3450237
(6, 1)				0/36639	0/877158	0/12124473
(4, 4)					0/32008	0/971824
(5, 3)					1/52560	28/1541010
(6, 2)					0/146100	0/4093944
(7, 1)					0/550914	0/14917146
(5, 4)						6/397195
(6, 3)						0/877977
(7, 2)						0/2534175
(8, 1)						0/9395415

Number of correctly predicted/number of all UIOs						
Partition \ UIO length	4	5	6	7	8	9
(2, 2)	14/14	42/42	132/132	429/429	1430/1430	4862/4862
(3, 1)	14/14	42/42	132/132	429/429	1430/1430	4862/4862
(3, 2)		42/42	132/132	429/429	1430/1430	4862/4862
(4, 1)		42/42	132/132	429/429	1430/1430	4862/4862
(3, 3)			132/132	429/429	1430/1430	4862/4862
(4, 2)			132/132	429/429	1430/1430	4862/4862
(5, 1)			132/132	429/429	1430/1430	4862/4862
(4, 3)				429/429	1430/1430	4862/4862
(5, 2)				429/429	1430/1430	4862/4862
(6, 1)				429/429	1430/1430	4862/4862
(4, 4)					1430/1430	4862/4862
(5, 3)					1429/1430	4842/4862
(6, 2)					1430/1430	4862/4862
(7, 1)					1430/1430	4862/4862
(5, 4)						4858/4862
(6, 3)						4862/4862
(7, 2)						4862/4862
(8, 1)						4862/4862

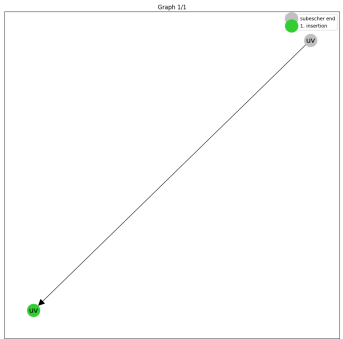


Table 1: Mismatch statistics for length 2 partitions for the model $[SEEnd < FirstIns]$, corresponding to the graph at bottom. Green entries indicate that this model gives lower bound for the Stanley coefficients even when mismatches occur.

Total absolute error/sum of real coefficients for all UIO						
Partition \ UIO length	4	5	6	7	8	9
(2, 1, 1)	0/16	0/256	0/2552	0/20304	0/141088	0/895072
(2, 2, 1)		0/42	0/860	0/10454	0/98088	0/784470
(3, 1, 1)		0/106	0/2052	0/23846	0/215620	0/1671830
(2, 2, 2)			0/108	0/2712	0/39216	0/427572
(3, 2, 1)			5/286	100/6872	1184/95536	10812/1006152
(4, 1, 1)			0/1024	0/23148	0/306112	0/3091580
(3, 2, 2)				0/742	0/21372	0/347850
(3, 3, 1)				16/1824	400/50940	5736/805620
(4, 2, 1)				68/3034	1503/82612	19623/1279950
(5, 1, 1)				0/12472	0/322284	0/4778064
(3, 3, 2)					54/4776	1560/156156
(4, 2, 2)					0/8344	0/267792
(4, 3, 1)					724/18758	20117/587564
(5, 2, 1)					1083/41706	25703/1265520
(6, 1, 1)					0/180144	0/5237856
(3, 3, 3)						0/28620
(4, 3, 2)						1173/51836
(4, 4, 1)						3236/177434
(5, 2, 2)						0/124470
(5, 3, 1)						12102/265838
(6, 2, 1)						17809/681792
(7, 1, 1)						0/2987556

Number of correctly predicted/number of all UIOs						
Partition \ UIO length	4	5	6	7	8	9
(2, 1, 1)	14/14	42/42	132/132	429/429	1430/1430	4862/4862
(2, 2, 1)		42/42	132/132	429/429	1430/1430	4862/4862
(3, 1, 1)		42/42	132/132	429/429	1430/1430	4862/4862
(2, 2, 2)			132/132	429/429	1430/1430	4862/4862
(3, 2, 1)			129/132	391/429	1157/1430	3359/4862
(4, 1, 1)			132/132	429/429	1430/1430	4862/4862
(3, 2, 2)				429/429	1430/1430	4862/4862
(3, 3, 1)				425/429	1369/1430	4344/4862
(4, 2, 1)				404/429	1202/1430	3493/4862
(5, 1, 1)				429/429	1430/1430	4862/4862
(3, 3, 2)					1416/1430	4651/4862
(4, 2, 2)					1430/1430	4862/4862
(4, 3, 1)					1309/1430	3824/4862
(5, 2, 1)					1268/1430	3662/4862
(6, 1, 1)					1430/1430	4862/4862
(3, 3, 3)						4862/4862
(4, 3, 2)						4593/4862
(4, 4, 1)						4625/4862
(5, 2, 2)						4862/4862
(5, 3, 1)						4144/4862
(6, 2, 1)						4068/4862
(7, 1, 1)						4862/4862

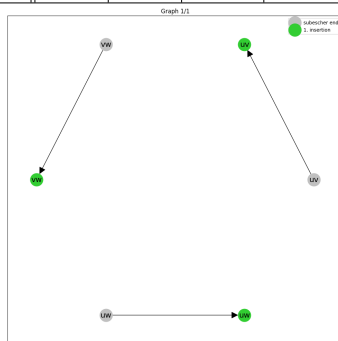


Table 2: Triple partitions: performance of the model $[SEEnd(u,v) < FirstIns(u,v)]$ AND $[SEEnd(v,w) < FirstIns(v,w)]$ AND $[SEEnd(u,w) < FirstIns(u,w)]$.

Total absolute error/sum of real coefficients for all UIO						
Partition \ UIO length	4	5	6	7	8	9
(2, 1, 1)	4/16	60/256	564/2552	4252/20304	28116/141088	170364/895072
(2, 2, 1)		10/42	196/860	2278/10454	20456/98088	156854/784470
(3, 1, 1)		52/106	960/2052	10676/23846	92656/215620	691364/1671830
(2, 2, 2)		0/108	0/2712	0/39216	0/427572	0/427572
(3, 2, 1)			178/286	4100/6872	54796/95536	556260/1006152
(4, 1, 1)			664/1024	14508/23148	185808/306112	1820580/3091580
(3, 2, 2)				454/742	12468/21372	194370/347850
(3, 3, 1)				834/1824	22572/50940	345780/805620
(4, 2, 1)				2026/3034	53292/82612	799206/1279950
(5, 1, 1)				9322/12472	234984/322284	3402364/4778064
(3, 3, 2)					2796/4776	87360/156156
(4, 2, 2)					4792/8344	147632/267792
(4, 3, 1)					15518/18758	475244/587564
(5, 2, 1)					35406/41706	1052460/1265520
(6, 1, 1)					146124/180144	4170312/5237856
(3, 3, 3)						0/28620
(4, 3, 2)						42764/51836
(4, 4, 1)						106218/177434
(5, 2, 2)						107670/124470
(5, 3, 1)						237488/265838
(6, 2, 1)						584256/681792
(7, 1, 1)						2550966/2987556

Number of correctly predicted/number of all UIOs						
Partition \ UIO length	4	5	6	7	8	9
(2, 1, 1)	12/14	27/42	58/132	121/429	248/1430	503/4862
(2, 2, 1)		39/42	101/132	242/429	545/1430	1174/4862
(3, 1, 1)		33/42	71/132	152/429	321/1430	673/4862
(2, 2, 2)			132/132	429/429	1430/1430	4862/4862
(3, 2, 1)			93/132	192/429	375/1430	715/4862
(4, 1, 1)			96/132	212/429	473/1430	1049/4862
(3, 2, 2)				398/429	1135/1430	3054/4862
(3, 3, 1)				381/429	1022/1430	2562/4862
(4, 2, 1)				261/429	518/1430	1028/4862
(5, 1, 1)				288/429	671/1430	1604/4862
(3, 3, 2)					1334/1430	3902/4862
(4, 2, 2)					1276/1430	3457/4862
(4, 3, 1)					956/1430	2131/4862
(5, 2, 1)					794/1430	1634/4862
(6, 1, 1)					895/1430	2210/4862
(3, 3, 3)						4862/4862
(4, 3, 2)						3948/4862
(4, 4, 1)						4122/4862
(5, 2, 2)						4160/4862
(5, 3, 1)						2839/4862
(6, 2, 1)						2556/4862
(7, 1, 1)						2894/4862

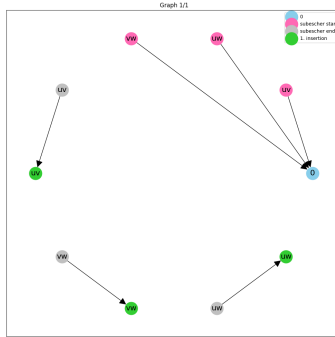


Table 3: Triple partitions with the model $[0 \geq \text{SEStart}(u,v)]$ AND $[0 \geq \text{SEStart}(u,w)]$ AND $[0 \geq \text{SEStart}(v,w)]$ AND $[\text{SEEnd}(u,v) < \text{FirstIns}(u,v)]$ AND $[\text{SEEnd}(v,w) < \text{FirstIns}(v,w)]$ AND $[\text{SEEnd}(u,w) < \text{FirstIns}(u,w)]$, giving lower bound for the Stanley coefficients

Total absolute error/sum of real coefficients for all UIO						
Partition \ UIO length	4	5	6	7	8	9
(1, 1, 1, 1)	0/24	0/384	0/3864	0/31224	0/221256	0/1435056
(2, 1, 1, 1)		0/66	0/1332	0/16158	0/152556	0/1234590
(2, 2, 1, 1)			0/180	0/4452	0/63976	0/698004
(3, 1, 1, 1)			0/456	0/10800	0/149676	0/1583436
(2, 2, 2, 1)				0/486	0/14316	0/239166
(3, 2, 1, 1)				28/1272	702/36148	10150/585036
(4, 1, 1, 1)				0/4608	0/124716	0/1936776
(2, 2, 2, 2)					0/1296	0/44352
(3, 2, 2, 1)					72/3476	2120/115596
(3, 3, 1, 1)					144/8648	4280/279956
(4, 2, 1, 1)					422/13804	11560/439024
(5, 1, 1, 1)					0/58728	0/1787232
(3, 2, 2, 2)						0/9306
(3, 3, 2, 1)						732/23864
(4, 2, 2, 1)						1058/39650
(4, 3, 1, 1)						5028/92456
(5, 2, 1, 1)						7176/193420
(6, 1, 1, 1)						0/886716
Number of correctly predicted/number of all UIOs						
Partition \ UIO length	4	5	6	7	8	9
(1, 1, 1, 1)	14/14	42/42	132/132	429/429	1430/1430	4862/4862
(2, 1, 1, 1)		42/42	132/132	429/429	1430/1430	4862/4862
(2, 2, 1, 1)			132/132	429/429	1430/1430	4862/4862
(3, 1, 1, 1)			132/132	429/429	1430/1430	4862/4862
(2, 2, 2, 1)				429/429	1430/1430	4862/4862
(3, 2, 1, 1)				420/429	1306/1430	3920/4862
(4, 1, 1, 1)				429/429	1430/1430	4862/4862
(2, 2, 2, 2)					1430/1430	4862/4862
(3, 2, 2, 1)					1415/1430	4620/4862
(3, 3, 1, 1)					1414/1430	4610/4862
(4, 2, 1, 1)					1347/1430	4054/4862
(5, 1, 1, 1)					1430/1430	4862/4862
(3, 2, 2, 2)						4862/4862
(3, 3, 2, 1)						4762/4862
(4, 2, 2, 1)						4730/4862
(4, 3, 1, 1)						4388/4862
(5, 2, 1, 1)						4290/4862
(6, 1, 1, 1)						4862/4862

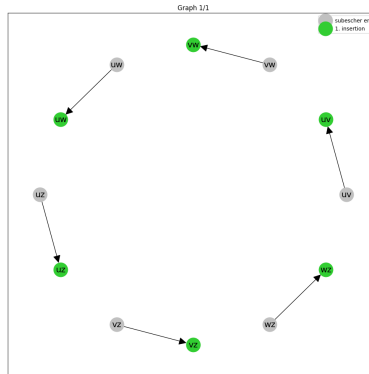


Table 4: Quadruple partition with the canonical model

Total absolute error/sum of real coefficients for all UIO						
Partition \ UIO length	4	5	6	7	8	9
(1, 1, 1, 1)	0/24	0/384	0/3864	0/31224	0/221256	0/1435056
(2, 1, 1, 1)		0/66	0/1332	0/16158	0/152556	0/1234590
(2, 2, 1, 1)			32/180	768/4452	10716/63976	113612/698004
(3, 1, 1, 1)			0/456	0/10800	0/149676	0/1583436
(2, 2, 2, 1)				84/486	2424/14316	39604/239166
(3, 2, 1, 1)				224/1272	6196/36148	97608/585036
(4, 1, 1, 1)				0/4608	0/124716	0/1936776
(2, 2, 2, 2)					0/1296	0/44352
(3, 2, 2, 1)					600/3476	19534/115596
(3, 3, 1, 1)					3086/8648	97728/279956
(4, 2, 1, 1)					2480/13804	76656/439024
(5, 1, 1, 1)					0/58728	0/1787232
(3, 2, 2, 2)						0/9306
(3, 3, 2, 1)						11384/23864
(4, 2, 2, 1)						7074/39650
(4, 3, 1, 1)						32014/92456
(5, 2, 1, 1)						35868/193420
(6, 1, 1, 1)						0/886716

Number of correctly predicted/number of all UIOs						
Partition \ UIO length	4	5	6	7	8	9
(1, 1, 1, 1)	14/14	42/42	132/132	429/429	1430/1430	4862/4862
(2, 1, 1, 1)		42/42	132/132	429/429	1430/1430	4862/4862
(2, 2, 1, 1)			123/132	338/429	882/1430	2232/4862
(3, 1, 1, 1)			132/132	429/429	1430/1430	4862/4862
(2, 2, 2, 1)				421/429	1314/1430	3934/4862
(3, 2, 1, 1)				393/429	1100/1430	2927/4862
(4, 1, 1, 1)				429/429	1430/1430	4862/4862
(2, 2, 2, 2)					1430/1430	4862/4862
(3, 2, 2, 1)					1371/1430	4172/4862
(3, 3, 1, 1)					1282/1430	3497/4862
(4, 2, 1, 1)					1238/1430	3308/4862
(5, 1, 1, 1)					1430/1430	4862/4862
(3, 2, 2, 2)						4862/4862
(3, 3, 2, 1)						4287/4862
(4, 2, 2, 1)						4531/4862
(4, 3, 1, 1)						4150/4862
(5, 2, 1, 1)						3955/4862
(6, 1, 1, 1)						4862/4862

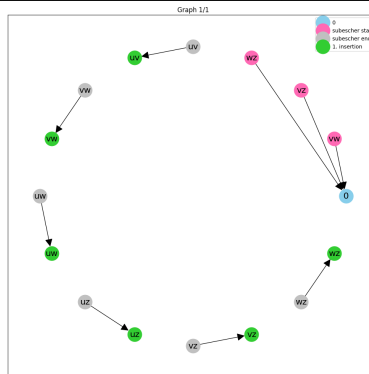


Table 5: Quadruple partitions with the modified canonical model, giving lower bound for the Stanley coefficients. Also the best conditions when allowing up to 6 additional conditions while only using the uv, uw, uz, vw, vz, wz subescher for the $[0 \geq \text{subescher start}]$ conditions

Total absolute error/sum of real coefficients for all UIO						
Partition \ UIO length	4	5	6	7	8	9
(2, 1, 1)	0/16	0/256	0/2552	0/20304	0/141088	0/895072
(2, 2, 1)		0/42	0/860	0/10454	0/98088	0/784470
(3, 1, 1)		0/106	0/2052	0/23846	0/215620	0/1671830
(2, 2, 2)			0/108	0/2712	0/39216	0/427572
(3, 2, 1)			4/286	80/6872	948/95536	8668/1006152
(4, 1, 1)			0/1024	0/23148	0/306112	0/3091580
(3, 2, 2)				0/742	0/21372	0/347850
(3, 3, 1)				16/1824	400/50940	5736/805620
(4, 2, 1)				48/3034	963/82612	11736/1279950
(5, 1, 1)				0/12472	0/322284	0/4778064
(3, 3, 2)					90/4776	2616/156156
(4, 2, 2)					0/8344	0/267792
(4, 3, 1)					644/18758	17877/587564
(5, 2, 1)					746/41706	15840/1265520
(6, 1, 1)					0/180144	0/5237856
(3, 3, 3)						0/28620
(4, 3, 2)						1380/51836
(4, 4, 1)						3236/177434
(5, 2, 2)						0/124470
(5, 3, 1)						9725/265838
(6, 2, 1)						13066/681792
(7, 1, 1)						0/2987556

Number of correctly predicted/number of all UIOs						
Partition \ UIO length	4	5	6	7	8	9
(2, 1, 1)	14/14	42/42	132/132	429/429	1430/1430	4862/4862
(2, 2, 1)		42/42	132/132	429/429	1430/1430	4862/4862
(3, 1, 1)		42/42	132/132	429/429	1430/1430	4862/4862
(2, 2, 2)			132/132	429/429	1430/1430	4862/4862
(3, 2, 1)			130/132	401/429	1209/1430	3566/4862
(4, 1, 1)			132/132	429/429	1430/1430	4862/4862
(3, 2, 2)				429/429	1430/1430	4862/4862
(3, 3, 1)				425/429	1369/1430	4344/4862
(4, 2, 1)				411/429	1248/1430	3679/4862
(5, 1, 1)				429/429	1430/1430	4862/4862
(3, 3, 2)					1406/1430	4526/4862
(4, 2, 2)					1430/1430	4862/4862
(4, 3, 1)					1317/1430	3886/4862
(5, 2, 1)					1306/1430	3848/4862
(6, 1, 1)					1430/1430	4862/4862
(3, 3, 3)						4862/4862
(4, 3, 2)						4588/4862
(4, 4, 1)						4625/4862
(5, 2, 2)						4862/4862
(5, 3, 1)						4193/4862
(6, 2, 1)						4164/4862
(7, 1, 1)						4862/4862

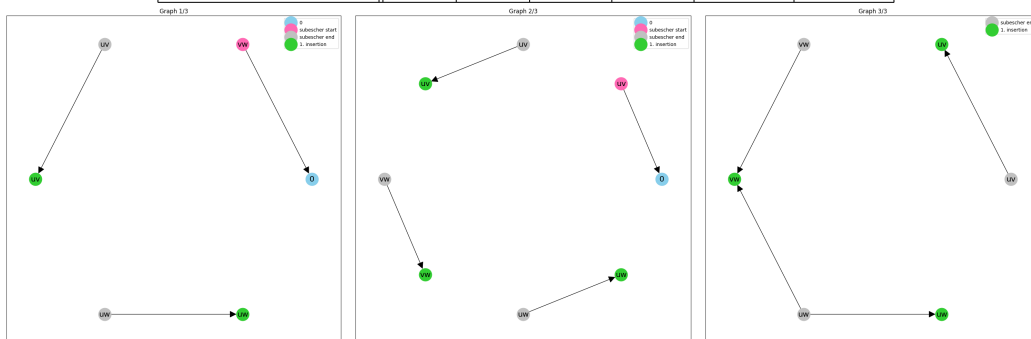


Table 6: A model with 3 condition graphs meaning the Boolean expression [graph1 OR graph2 OR graph3]. It is trained on (5, 2, 1) partition with 9 intervals, and shows that the RL agent often finds better conditions for individual partitions.

Total absolute error/sum of real coefficients for all UIO						
Partition \ UIO length	4	5	6	7	8	9
(1, 1, 1, 1)	0/24	0/384	0/3864	0/31224	0/221256	0/1435056
(2, 1, 1, 1)		0/66	0/1332	0/16158	0/152556	0/1234590
(2, 2, 1, 1)			32/180	768/4452	10716/63976	113612/698004
(3, 1, 1, 1)			0/456	0/10800	0/149676	0/1583436
(2, 2, 2, 1)				84/486	2424/14316	39604/239166
(3, 2, 1, 1)				224/1272	6196/36148	97608/585036
(4, 1, 1, 1)				0/4608	0/124716	0/1936776
(2, 2, 2, 2)					0/1296	0/44352
(3, 2, 2, 1)					600/3476	19534/115596
(3, 3, 1, 1)					3086/8648	97728/279956
(4, 2, 1, 1)					2480/13804	76656/439024
(5, 1, 1, 1)					0/58728	0/1787232
(3, 2, 2, 2)						0/9306
(3, 3, 2, 1)						11384/23864
(4, 2, 2, 1)						7074/39650
(4, 3, 1, 1)						32014/92456
(5, 2, 1, 1)						35868/193420
(6, 1, 1, 1)						0/886716

Number of correctly predicted/number of all UIOs						
Partition \ UIO length	4	5	6	7	8	9
(1, 1, 1, 1)	14/14	42/42	132/132	429/429	1430/1430	4862/4862
(2, 1, 1, 1)		42/42	132/132	429/429	1430/1430	4862/4862
(2, 2, 1, 1)			123/132	338/429	882/1430	2232/4862
(3, 1, 1, 1)			132/132	429/429	1430/1430	4862/4862
(2, 2, 2, 1)				421/429	1314/1430	3934/4862
(3, 2, 1, 1)				393/429	1100/1430	2927/4862
(4, 1, 1, 1)				429/429	1430/1430	4862/4862
(2, 2, 2, 2)					1430/1430	4862/4862
(3, 2, 2, 1)					1371/1430	4172/4862
(3, 3, 1, 1)					1282/1430	3497/4862
(4, 2, 1, 1)					1238/1430	3308/4862
(5, 1, 1, 1)					1430/1430	4862/4862
(3, 2, 2, 2)						4862/4862
(3, 3, 2, 1)						4287/4862
(4, 2, 2, 1)						4531/4862
(4, 3, 1, 1)						4150/4862
(5, 2, 1, 1)						3955/4862
(6, 1, 1, 1)						4862/4862

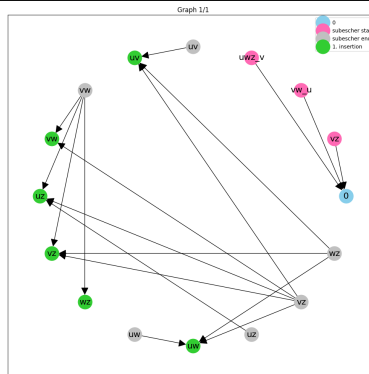


Table 7: A model found by the RL agent for quadruple partitions with only negative errors, and with better performance than the model of Theorem 3. This shows that graphs which give lower bound for the Stanley coefficients are not unique, but finding one with general pattern is harder.

6 Analysis of the Machine Learning Method

The machine learning approach we employed to tackle this problem presented several notable challenges. Below, we outline key observations and strategies that emerged during the process, along with the implications for optimizing the training process.

6.1 Non-Uniqueness of Solutions and Balancing Complexity

For most partition types, there is no single best solution. Even when a perfect solution (i.e., a solution that achieves a zero-error score) is found, the corresponding condition graph is often not unique. Table 2 and 6 illustrate this for the case of the partition (a, b, b) . This observation indicates the need to balance between obtaining optimal solutions with potentially highly complex condition graphs and accepting slightly suboptimal solutions that correspond to significantly simpler, more interpretable, and potentially more universal condition graphs. This trade-off between accuracy and simplicity is critical to the applicability and generalization of our model.

6.2 Managing the Comparison Space

As the size of the partition grows, the comparison space becomes exponentially large, leading to impractical memory requirements during training. For example, training the model for partitions of length greater than five quickly exhausts available resources. To mitigate this, we must reduce the comparison space, which necessitates leveraging mathematical intuition. By identifying symmetries and reducing redundant comparisons, we can make the search space more tractable while still preserving solution quality.

6.3 Training Pitfalls in Large Search Spaces

One of the common pitfalls in training with a large comparison space is the lack of satisfying solutions for random Boolean expressions. In many cases, none of the Escher tuples meet the given conditions after the initial random iteration, causing the model to become trapped in a suboptimal region where the best achievable score is merely the sum of the nonzero Stanley coefficients across all UIOs. To avoid this, we must guide the training process to prevent such stagnation, ensuring that the model does not get trapped in these non-productive domains.

6.4 Reducing Cores and Comparisons

An essential aspect of optimizing the model involves reducing the number of cores and comparisons. For example, in the case of $n = 3$, the optimal solution only utilizes specific cores (e.g., *SEEnd* and *FirstIns*), while others, such as 0 and *SEStart*, are not used. This insight suggests that for $n = 4$, we can eliminate the *SEStart* cores and restrict

comparisons to pairs of cores such as $(0, SEStart)$ and $(SEEnd, FirstIns)$. This reduction in action space helps prevent the model from being stuck in local minima during training, significantly improving efficiency.

6.5 Core Selection and Encoding Decision Trees

The process of selecting the appropriate cores is critical to model performance. Encoding decision trees with graphs is a complex task, and it took several months to identify the correct core vectors. Specifically, interpreting the meaning of expressions like $\mathbf{SEEnd}(u, v) < \mathbf{FirstIns}(u, v)$ requires a deep understanding of multiple aspects of the graph’s structure. These core vectors play a crucial role in ensuring that the model captures the right relationships between the nodes and edges of the decision tree.

6.6 Condition Graph Row Selection

Another critical factor in the model’s design is the number of rows used in the condition graph. In theory, adding a second row expands the search space to include solutions that require only one row. However, in practice, increasing the number of rows dramatically increases the state space, which, in turn, heightens the risk of the model becoming stuck in good-but-not-optimal solutions. Through experimentation, we found that solutions using 1-3 rows often outperformed those with more rows, even though a larger state space theoretically allows for more complex solutions.

6.7 Importance of the Score Function

The choice of score function is pivotal in guiding the reinforcement learning (RL) agent toward optimal solutions. In particular, the role of the edge penalty is crucial. We observed that when $\text{EdgePenalty} > 1$, the RL agent tends to prioritize shorter solutions, i.e., smaller condition graphs, at the expense of better absolute error. Through extensive experimentation, we determined that the optimal range for EdgePenalty lies between 0.1 and 0.5. This range strikes a balance between solution length and accuracy, leading to more efficient exploration of the solution space.

6.8 Training charts

We added a `ResultViewer` folder to the GitHub repository, where the reinforcement training process is monitored and saved as charts. An example is shown in Figure 4.

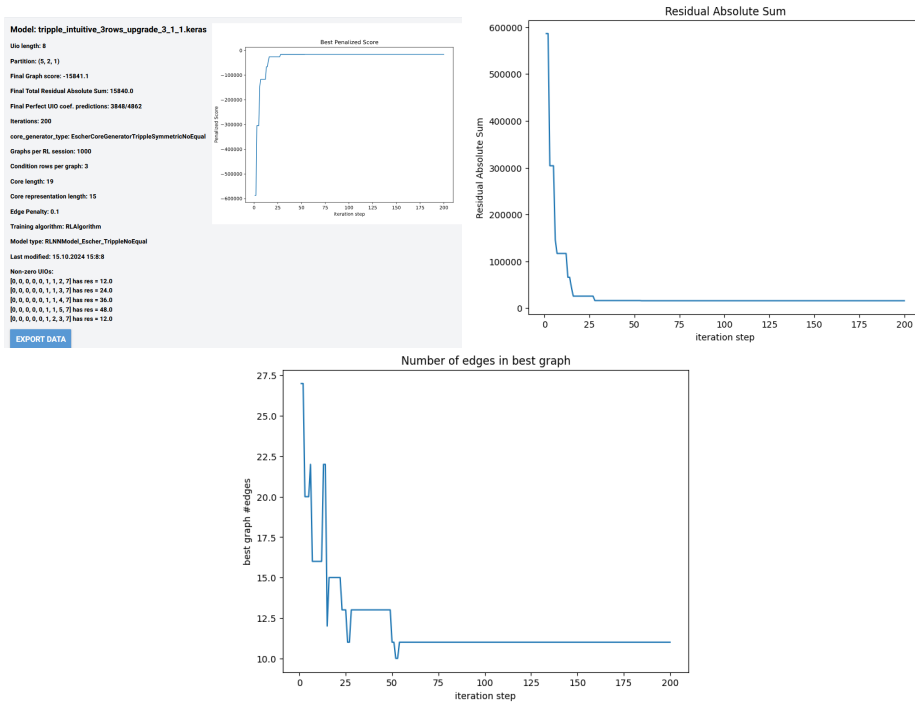


Figure 4: Training charts for the partition $(5, 2, 1)$ trained on all UIOs of length 8, with 3 rows in the condition graph. The number of correctly predicted coefficients is $3848/4862$. Because EdgePenalty_1 , the model occasionally adds edges to the condition graph to achieve a lower total score, resulting in jumps in the number of edges.

7 Using different ML models

A promising machine learning approach to determining Stanley coefficients is to apply a supervised learning model. This idea is attractive for several reasons:

1. The input data consists of a sequence of n unit intervals on a line, and the corresponding unit interval graph can be encoded as an increasing sequence of n integers between 0 and $n - 1$, also called the area sequence.
2. The output is a series of integer coefficients. With the right model, saliency analysis can be performed to identify which features of the Unit Interval Orders (UIOs) influence a particular coefficient.

We experimented with various feed-forward neural networks as well as small BERT-type GPT models, utilizing encoder transformers with full attention. This method has two significant limitations: (1) The training set is limited. Computing Stanley coefficients for

UIOs is computationally expensive, requiring substantial memory, and we are constrained to sequences of length around 10. (2) While feature analysis is possible, it doesn't provide a true explanation for the coefficients. However, recent advances in the mathematical interpretability of transformer models have prompted us to explore this avenue in our ongoing research.

References

- [1] M. Guay-Paquet. A modular law for the chromatic symmetric functions of $(3 + 1)$ -free posets. arXiv:1306.2400, 2013.
- [2] Gurobi Optimization, LLC. Gurobi Optimizer Reference Manual, 2024.
- [3] T. Hikita. A proof of the stanley-stembridge conjecture. *arXiv preprint arXiv:2410.12758*, 2024. <https://arxiv.org/abs/2410.12758>.
- [4] J. Huh. Milnor numbers of projective hypersurfaces and the chromatic polynomial of graphs. *Journal of the American Mathematical Society*, 25:907–927, 2012.
- [5] I. Macdonald. *Symmetric Functions and Hall Polynomials*. Oxford University Press, Oxford, 1979.
- [6] D. Scott and P. Suppes. Foundational aspects of theories of measurement. *Journal of Symbolic Logic*, 23:113–128, 1954.
- [7] J. Shareshian and M. L. Wachs. Chromatic quasisymmetric functions. *Advances in Mathematics*, 295(4):497–551, June 2016.
- [8] R. P. Stanley. A symmetric function generalization of the chromatic polynomial of a graph. *Advances in Mathematics*, 111(1):166–194, 1995.
- [9] R. P. Stanley. Graph colorings and related symmetric functions: ideas and applications. *Discrete Mathematics*, 193(1):267–286, 1998.
- [10] R. P. Stanley and J. R. Stembridge. On immanants of jacobi–trudi matrices and permutations with restricted position. *Journal of Combinatorial Theory, Series A*, 62(2):261–279, March 1993.
- [11] A. Szenes and A. Rok. Eschers and Stanley's chromatic e-positivity conjecture in length-2. arXiv:2305.00963, 2023.
- [12] A. Z. Wagner. Constructions in combinatorics via neural networks. arXiv:2104.14516, 2021.